 

*CONTROL OF LASER RADIATION PARAMETERS*

https://doi.org/10.1070/QEL17569

# Passive method of laser radiation smoothing using spectral dispersion

D.V. Sizmin, V.N. Pugacheva, K.V. Starodubtsev, L.A. Dushina,
O.I. Gorchakov, V.N. Derkach, I.N. Voronich

***Abstract.*** **A new version of the method for spatiotemporal smoothing of laser radiation using spectral dispersion is proposed, which does not require the use of high-frequency phase modulators, i.e. a method based on the use of a broadband master oscillator. An experimental study of this method has been conducted on the Luch laser facility.**

***Keywords:*** *smoothing of laser radiation, spectral dispersion, uniformity of target irradiation, partially coherent radiation, speckles.*

## 1. Introduction

High uniformity of target irradiation is a necessary condition for fuel ignition in laser thermonuclear fusion. Large-scale inhomogeneity of irradiation causes the occurrence and development of hydrodynamic instabilities that do not allow a high degree of thermonuclear fuel compression to be achieved; the presence of small-scale inhomogeneities (speckles) leads to the development of parametric instabilities, generation of hot electrons, and premature heating of the fuel. Therefore, in the case of direct irradiation of a target, the irradiation inhomogeneity should not exceed 1%–2% [1].

On high-power Nd:glass laser facilities intended for research in the field of laser thermonuclear fusion, such as NIF, Omega, LMJ, the speckled structure of radiation on the target is smoothed by the spectral dispersion method (smoothing by spectral dispersion, SSD). The essence of the method is that radiation of the master oscillator passes through a phase modulator and a spectral dispersion element (diffraction grating) [2]. In the spectral-angular representation, the phase modulator broadens the pulse spectrum, and the diffraction grating separates the spectral components of the radiation at different angles. As a result, the radiation intensity in the target plane (in the far field) is a superposition of a set of speckled distributions shifted in the transverse direction, which leads to a decrease in the contrast of the total distribution. In the spatiotemporal representation, radiation that has passed the phase modulator acquires phase oscillations $\varphi(t)$, and the grating forms a slope along the aperture of the beam front with a delay $\tau_d$ in the transverse direction, which occurs due to the difference in the angles of incidence and reflection during diffraction in the nonzero order. The phase becomes nonstationary both in time and in the coordinate: $\varphi(t, y)$, which results in a change in the speckled distribution of the beam on the target in time. Smoothing occurs when a large number of independent random intensity distributions are averaged over the time of the plasma's hydrodynamic response. To exclude the broadening of pulse fronts due to the spatiotemporal slope, an additional diffraction grating can be introduced into the SSD circuit in front of the phase modulator, introducing a delay of the opposite sign (Fig. 1a).

**D.V. Sizmin, V.N. Pugacheva, K.V. Starodubtsev, L.A. Dushina, O.I Gorchakov, V.N. Derkach, I.N. Voronich** Russian Federal Nuclear Center–All-Russian Scientific Research Institute of Experimental Physics (RFNC-VNIIEF), prosp. Mira 37, 607188 Sarov, Nizhny Novgorod region, Russia;
e-mail: oefimova@otd13.vniief.ru; seazmin@yandex.ru

Received 19 April 2021
*Kvantovaya Elektronika* **51** (8) 683–686 (2021)
Translated by M.A. Monastyrskiy

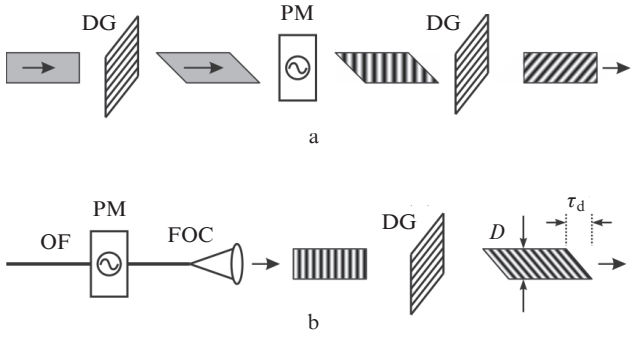


**Figure 1.** Scheme of a one-dimensional SSD (a) with temporal slope precompensation and (b) with a fibre-optic phase modulator and a single diffraction grating:
(DG) diffraction grating; (PM) phase modulator; (OF) optical fibre; (FOC) fibre-optic collimator.

A signal $E(t)$ with a carrier frequency $\omega_0$, sinusoidal phase modulation with frequency $\omega_M$, and depth $\delta$,

$$E(t) = E_0 \exp(i\omega_0 t + i\delta\omega_M t), \tag{1}$$

has a spectrum consisting of equidistant lines with an interval $\omega_M$:

$$E(t) = E_0 e^{i\omega_0 t} \sum_{n=-\infty}^{\infty} J_n(\delta) \exp(in\omega_M t); \tag{2}$$

thus, only the spectral components in the interval $\pm(\delta + 1)\omega_M$ have a significant intensity, which gives an estimate of the spectral width $\Delta\omega \approx 2(\delta + 1)\omega_M$. After passing through a grating with angular dispersion $\partial\theta/\partial\lambda$, phase modulation occurs in the direction of the transverse coordinate $y$:

$$E(t, y) = E_0\exp[i\omega_0 t + i\delta\sin(\omega_M t + \alpha y)], \quad (3)$$

where $\alpha$ is the spatial frequency of transverse phase oscillations, defined as

$$\alpha = 2\pi\frac{\omega_M}{\omega_0}\frac{\partial\theta}{\partial\lambda}. \quad (4)$$

The transverse time delay is

$$\tau_d = \frac{\lambda D}{c}\frac{\partial\theta}{\partial\lambda}. \quad (5)$$

It is possible to increase the smoothing efficiency by using the dispersion in two coordinates. To this end, a pair of diffraction gratings oriented perpendicular to the first pair, with a second phase modulator between them, should be added to the scheme shown in Fig. 1a.

The SSD scheme with precompensation of the spatiotemporal slope, and especially the scheme with two-dimensional dispersion, requires the use of special high-frequency phase modulators with an aperture of several millimetres. In modern installations, the initial part of the front end system is based on fibre elements, and so commercially available integrated optical phase modulators with a modulation frequency of tens of GHz can be used for SSD. Figure 1b shows a schematic of the SSD system used on the Omega-EP and NIF installations in experiments with direct target irradiation. However, in this configuration, smoothing only occurs in a single direction, and the roll-off of the pulse fronts remains uncompensated during the time $\tau_d$.

The periodic nature of single-frequency modulation leads to the presence of an asymptotic level of radiation contrast on the target and, consequently, to a relatively small smoothing, since the beam phase reproduces its shape in a time $T = 2\pi/\omega_M$, and due to the spectrum discreteness, the irradiation inhomogeneity for part of the spatial frequencies is not smoothed at all. These disadvantages can be eliminated if multi-frequency phase modulation is applied at specially selected non-multiple frequencies. For example, on the Omega-EP installation, the modulation is performed at three frequencies: 21.2, 22.8, and 31.9 GHz with amplitudes of 0.45, 1.04, and 2.07, respectively, which results in a third harmonic spectrum width of ~0.5 THz with an aperture delay of $\tau_d = 245$ ps [3].

When using the SSD method, unlike other smoothing methods, the laser radiation in the amplifying path is not intensity-modulated (although in this case, special measures must be taken to prevent the transition of phase modulation to amplitude modulation); this is important for high-power installations operating in high fluence regimes near the damage threshold. Another advantage of the method is the possibility of efficient conversion of broadband radiation into the third harmonic; in this case, the magnitude and direction of the spectral dispersion are made consistent with the dispersion of the phase-matching angle in the converter crystal.

We have proposed a passive version of the smoothing by spectral dispersion, in which radiation of the master oscillator (MO) itself has a wide spectrum, which makes it possible not to use microwave phase modulators. The advantage of this method is the simplicity of implementation, a large spectral width, and the absence of an asymptotic contrast level on the target. The intermode distance of the output radiation spectrum is 3–4 orders of magnitude less than the MO spectrum width; thus, its spectrum can be considered quasi-continuous, i.e. smoothing of the laser radiation inhomogeneity on the target occurs in a wide range of spatial frequencies.

## 2. Scheme and conditions of experiments

A scheme of the front end system is shown in Fig. 2. An electro-optically $Q$-switched, flash-lamp-pumped master oscillator on a neodymium phosphate glass with a flat resonator has a spectral width of 2 nm at a level of 0.5, and 5.4 nm at a level of 0.01 (0.54 and 1.46 THz, respectively); the pulse duration is 17 ns at a centre wavelength of 1054.2 nm. The MO spectrum recorded by the high-resolution Solar LS SHR spectrometer ($\lambda/\Delta\lambda = 30000$) is shown in Fig. 3. After passing through a single-pass preamplifier PA1, the MO radiation enters the Pockels gate, which cuts out a 5 ns pulse and serves as a decoupling between the preamplifier stages. Next, the pulse is amplified in the second (two-pass) preamplifier PA2 and reflected from the diffraction grating (1200 lines mm$^{-1}$) located at an angle close to the Littrow angle of 39°. The diffraction efficiency of the grating in the –1st order is ~70%.

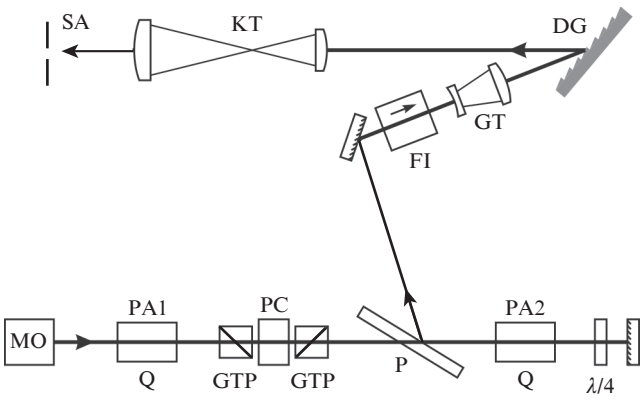


**Figure 2.** Scheme of the reference radiation formation system with passive spectral smoothing:
(MO) master oscillator; (PA1, PA2) preamplifiers; (Q) quantron; (GTP) Glan–Taylor prism; (PC) Pockels cell; (P) polariser; ($\lambda$/4) quarter-wave phase plate; (FI) Faraday insulator; (GT) Galileo telescope; (DG) diffraction grating; (KT) Kepler telescope; (SA) serrated aperture.

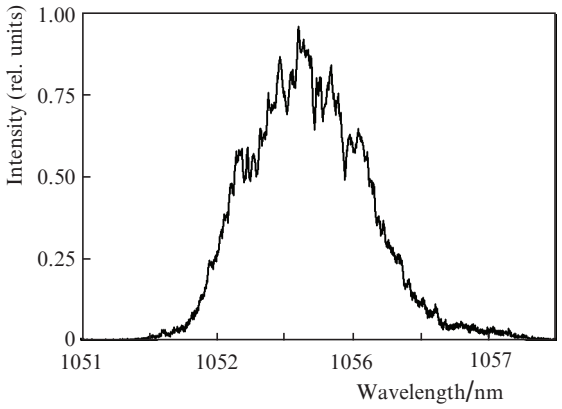


**Figure 3.** Master oscillator spectrum.

After passing the diffraction grating, the radiation beam, magnified by the Kepler telescope (KT), enters the system for forming a square apodised beam profile, consisting of a serrated aperture and a spatial filter, and then arrives at the input of the main amplifying channel of the Luch facility [4].

The size of the beam incident on the grating (1 cm) was chosen in such a way that the angular size of the radiation in the channel (after magnification by a factor M = 36)

$$\Delta\theta = \frac{1}{M}\frac{\partial\theta}{\partial\lambda}\Delta\lambda \tag{6}$$

was less than the minimum angular aperture of the spatial filters in the path, equal to 300 mrad.

At $\partial\theta/\partial\lambda = 1.55 \times 10^{-3}$ rad nm$^{-1}$ and $\Delta\lambda = 5.4$ nm, we have $\Delta\theta = 225$ mrad. In this case, the time shift is $\tau_d = 53$ ps, which is negligible from the viewpoint of pulse broadening, but 30 times higher than the coherence time.

The radiation dispersion was introduced in the direction of polarisation, i.e., orthogonal to the matching plane of the KDP crystal – a converter to the second harmonic, which is located at the amplifying channel output and operates with type-I phase matching. This circumstance, as well as the large spectral width of the second harmonic generation matching in the KDP crystal ($\partial\Delta k/\partial\lambda = 0.18$ cm$^{-1}$ nm$^{-1}$) provided a relatively high conversion coefficient of the fundamental frequency into the second harmonic without taking any special measures.

## 3. Experimental results

A series of experiments on the amplification of smoothed radiation and its conversion into the second harmonic was performed on the Luch laser facility. At the channel output, the pulse energy of the first harmonic up to 756 J at a beam size of 18 × 18 cm was obtained, with a technical coefficient of conversion to the second harmonic up to 32% (a ratio of the pulse energy at a frequency $2\omega$ at the nonlinear crystal output to the energy of a pulse with a frequency $\omega$, incident on the crystal), and a pulse duration of 4 ns. Both the gain and the conversion efficiency of smoothed radiation virtually do not differ from those for unsmoothed radiation at given intensity values.

Figure 4 shows the time-integrated images of the beam incident on the target (using a lens raster and an objective lens with $F = 100$ cm forming a rectangular spot approximately 600 × 300 μm in size), recorded in an equivalent plane.

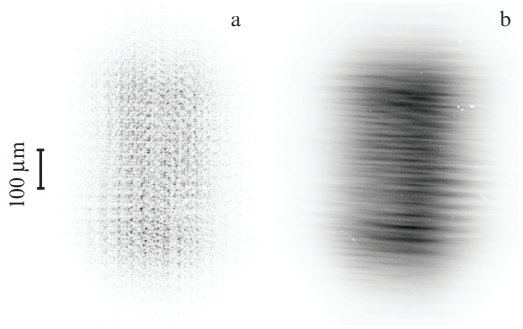


**Figure 4.** Energy density distributions on the target (a) by using coherent radiation from the standard front end system of the Luch facility and (b) by using a passive SSD.

To evaluate the efficiency of one-dimensional smoothing at various spatial frequencies, the spatial spectra of the energy density distributions $Q(x, y)$ shown in Fig.4 were calculated. To this end, the square of the modulus of the discrete two-dimensional Fourier transform (FFT) of the function $Q(x, y)$ was averaged over the vertical coordinate:

$$S(\nu_x) \propto \int S(\nu_x, \nu_y)\mathrm{d}\nu_y,$$

$$\text{where } S(\nu_x, \nu_y) = |\mathrm{FFT}\{Q(x, y)\}|^2. \tag{7}$$

The $S(\nu_x)$ dependences for the unsmoothed and smoothed radiation are shown in Fig. 5. The small-scale inhomogeneity (with a characteristic size of less than 100 μm) in the horizontal direction was reduced by 2–3 orders of magnitude for the smoothed spot compared to the non-smoothed one.

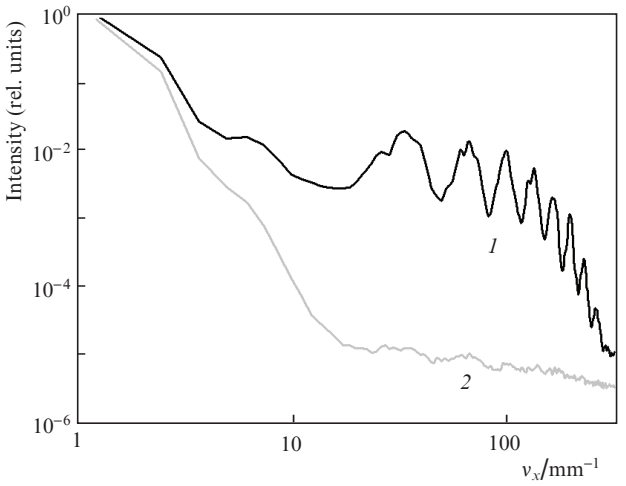


**Figure 5.** One-dimensional spatial spectrum of the energy density distribution on the target along the horizontal axis for (*1*) unsmoothed and (*2*) smoothed radiation.

The energy density contrast (the ratio of the root-mean-square deviation to the mean value) in the central part of the spot is 65.2% for unsmoothed radiation and 22.3% for smoothed radiation. In the high-frequency part of the spectrum (at $\nu > 100$ mm$^{-1}$), the contrast is 61.4% and 9.52%, respectively, while the average contrast of the one-dimensional distribution along the horizontal axis is 58.2% and 2.76%.

The sweep view of the horizontal cross section of the smoothed radiation intensity distribution on the target (Fig. 6) indicates a rapid change in the position of speckles along the $x$ axis. However, the true rate the speckled pattern rearrangement cannot be estimated from this recording, since the temporal resolution (~70 ps) of the streak camera used [5] is not sufficient to record changes occurring during the laser radiation coherence time (~0.9 ps at the second harmonic).

## 4. Conclusions

A new version of the method of one-dimensional spatiotemporal smoothing of laser radiation by spectral dispersion is proposed and implemented – the version is based on the use of a broadband master oscillator. An advantage of this

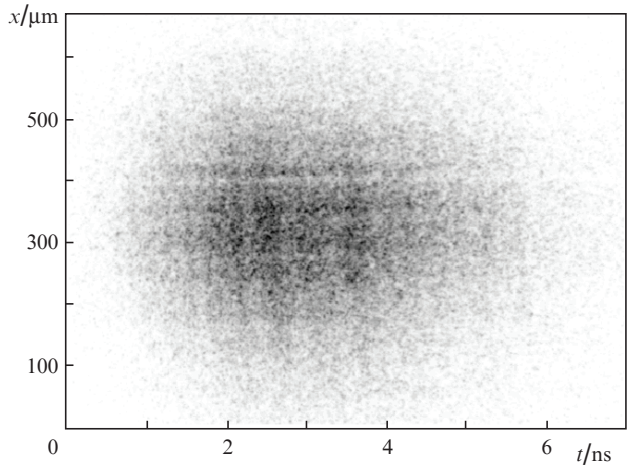


**Figure 6.** Streaked image of the horizontal cross section of the spot shown in Fig. 4b.

method is a wide radiation spectrum, which is difficult to attain when using phase modulators, and, as a result, a short coherence time (accordingly, a rapid rearrangement of the speckled intensity distribution on the target), as well as the possibility of using a diffraction grating with a lower dispersion, which entails lesser spreading of the pulse fronts due to the spatiotemporal shift. It is important that the emission spectrum of the broadband MO is quasi-continuous, rather than discrete, as in the case of using a phase modulator. The consequence of this is a high degree of smoothing (the absence of an asymptotic contrast level), as well as its uniformity in the small-scale part of the spatial spectrum of the spot in the far field.

Experiments on the generation, amplification and conversion to the second harmonic of partially coherent radiation with passive SSD have been performed on the Luch laser facility. The gain and conversion coefficients do not differ from the corresponding coefficients for the coherent radiation of the master oscillator of the facility. Smoothing resulted in a 6.5-fold decrease in the contrast of the small-scale part of the two-dimensional energy density distribution on the target, and a 20-fold decrease in the contrast of the one-dimensional distribution (along the direction of dispersion).

To take full advantage of the SSD method, it is necessary to design a broadband master oscillator with controlled spatiotemporal characteristics, in which the spectrum width arises due to random phase oscillations rather than to amplitude oscillations. The solution to this problem can become an obstacle in the implementation of the described method of passive smoothing in comparison with the use of microwave phase modulators.

## References

1. Skupsky S., Craxton R.S. *Phys. Plasmas*, **6**, 2157 (1999).
2. Skupsky S., Short R.W., Kessler T., et al. *J. Appl. Phys.*, **66**, 3456 (1989).
3. Hohenberger M., Shvydky A., Marozas J.A., et al. *Phys. Plasmas*, **23**, 092702 (2016).
4. Garanin S.G., Zaretskii A.I., Il'kaev R.I., et al. *Quantum Electron.*, **35**, 299 (2005) [*Kvantovaya Electron.*, **35**, 299 (2005)].
5. Kornienko D.S., Kravchenko A.G., Litvin D.N., et al. *Prib. Tekh. Eksp.*, **2**, 79 (2014).